High Precision Optical Measurement of Carrier Mobilities Using Z-scan Photo-modulated Reflectance

Will Chism[1, a)]
Xitronix Corporation, 106 E. Sixth St., Ninth Floor, Austin, TX, USA 78701

(Dated: 29 January 2018)

A simple yet precise optical technique for measuring electronic mobility in semiconductors is presented. Using tightly focused Gaussian laser beams in a photo-modulated reflectance system, the modulated reflectance signal is measured as a function of the longitudinal (Z) displacement of the sample from focus. The modulated component of the reflected probe beam is also a Gaussian beam with its profile determined by the focal parameters and the complex diffusion length. The reflected probe beam is collected and input to the detector, thereby integrating over the radial profile of the beam. This results in analytic expressions for the Z dependence of the photo-modulated reflectance signal in terms of carrier diffusion length and recombination lifetime. Best fit values for the diffusion length and recombination lifetime are obtained via a nonlinear regression analysis. The output diffusion lengths and recombination lifetimes and their estimated uncertainties are combined according to the Einstein relation to yield the electronic mobility and its uncertainty.

I. INTRODUCTION

Semiconductor device performance depends fundamentally on the mobility of charge carriers within the semiconductor. In modern semiconductor device manufacturing, many process steps have the potential to alter or degrade carrier mobility, resulting in device timing variability and loss of manufacturing yield. Such systematic process variability is best addressed by measurements made directly on product wafers between processing steps. However, at present, process control for carrier transport parameters is commonly implemented on sacrifical wafers using destructive four-point probe (4PP) and/or Hall effect measurements. Even the most advanced "micro-4PP" and "micro-Hall" techniques require contact with the sample. Thus the capability to measure the carrier mobility in a non-contact manner, between process steps, remains an outstanding need.

Optical techniques are ideal for process control of semiconductor manufacturing as they are non-contact, can be performed rapidly, and may provide micrometer scale resolution. Numerous optical techniques have been developed for measurement of carrier electronic properties. Surface photovoltage (SPV),[1,2] photoconductance decay,[3] free carrier absorption,[3] photoluminescence,[4] and time-resolved THz spectroscopy[5,6] are among the techniques frequently reported. However, none of these techniques have the speed and/or spatial resolution required to measure carrier mobility between processing steps. For example, the last technique, THz spectroscopy, is sensitive to mobility but requires a complex and expensive experimental setup.

In this letter, a simple yet precise optical technique for measuring the ambipolar carrier mobility in semiconductors is demonstrated. The technique is based upon profiling of the output signals of a photo-modulated reflectance (PMR) system as the sample is stepped through focus. The system uses Gaussian laser beams for both the pump and probe beams. Simple analytic expressions for the Z-profile of the PMR signal are used in a nonlinear regression analysis to provide best fit diffusion lengths and recombination lifetimes. The carrier mobility may then be determined via the Einstein relation.

To demonstrate this technique, referred to as Z-scan PMR, parameterized expressions for the Z dependence of the PMR signal amplitude and phase were fit to experimental Z-scan PMR data obtained from a set of samples consisting of p-type ultra-shallow junctions formed in silicon using advanced ion implantation and annealing processes. Independent estimates of the near surface diffusion length and recombination lifetime were obtained from the fit procedure. Statistical estimates of fit error were used to estimate precision of the determined diffusion lengths and recombination lifetimes. These values were used to determine the mobility and its precision via the Einstein relation. Systematic effects of process variations on carrier electronic properties are observed. For the optical mobility measurements reported here, estimated uncertainties in the mobility remain less than 2%.

II. THE Z-SCAN PMR TECHNIQUE

In PMR,[7] an intensity modulated pump light beam is used to photo-inject charge carriers in a semiconductor sample while a second probe light beam is used to detect the modulated reflectance of the sample. Lock-in amplification is used to suppress unwanted noise, resulting in the ability to detect ppm level reflectance changes. As noted, the technique here uses Gaussian laser beams for both the pump and probe beams. The beams are collinear and co-focused to a point along the beam path. Z is the displacement of the sample from the common beam waist along the focal column. The reflected probe beam is collected and input to the detector, thereby integrating over the radial profile of the beam. The detector

[a)] Electronic mail: wchism@xitronixcorp.com

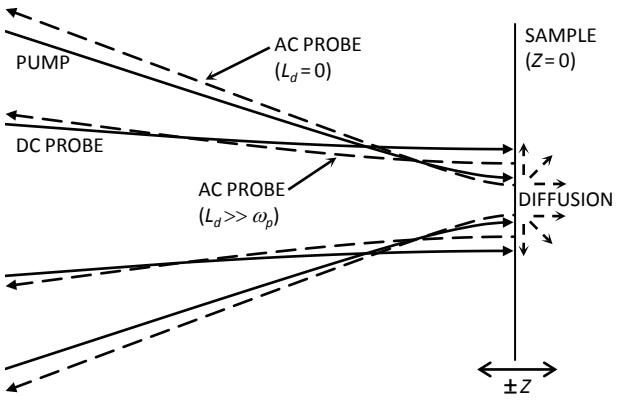

FIG. 1. Representative cross-section of beams present in the Z-scan PMR system. The reflected AC probe beam profile is highly sensitive to L_d.

output is passed to the lock-in amplifier, which measures the PMR signal. The acquired Z-scan PMR signal is the relative change in the radially integrated reflected probe light intensity and consists of a vector characterized by an amplitude and a phase. The amplitude is the induced AC change in reflectance divided by the linear (DC) reflectance, whereas the phase characterizes the temporal delay of the reflectance change due to the relaxation dynamics of the carriers within the sample. The sample is stepped through focus and the integrated PMR signal is acquired sequentially as a function of Z.

The focal geometry of the incident pump and probe beams at $Z = 0$ is illustrated in Fig. 1. At focus, the linear reflected pump and probe beam profiles will coincide with their respective input beam profiles. The pump will induce a reflectance modulation within a radius $\omega_m \equiv (\omega_p^2 + L_d^2)^{1/2}$, where ω_p is the pump beam waist and L_d is the carrier diffusion length.[8] Therefore, as the sample is stepped through focus the area of modulation varies according to $\omega_m^2(Z) = \omega_p^2(Z) + L_d^2$, where $\omega_p^2(Z) = \omega_p^2[1 + (Z/z_p)^2]$, $z_p = \pi\omega_p^2/\lambda_p$, and λ_p is the pump beam wavelength. The modulated component of the reflected probe beam is also a Gaussian beam with its radius defined by the incident probe beam radius and the (diffusion dependent) radius of modulation. Thus a new reflected AC beam profile will be generated for each value of Z. Fig. 1 also shows the reflected AC probe beam profile for different values of L_d. When $L_d \cong 0$, the effective waist of the AC reflected probe beam is smaller than the waist of the DC probe beam. However, when $L_d^2 \gg \omega^2$ the AC reflected probe beam will approach the linear reflected probe beam profile. Integrating over the radial dependence of the reflected DC and AC beams results in simple analytic expressions for the Z dependence of the PMR amplitude and phase in terms of carrier diffusion length and recombination lifetime. A straightforward parametrization of the analytic expressions enables these carrier parameters to be determined via nonlinear regression on the Z-scan PMR phase and amplitude data. The mobility may then be obtained from the Einstein relation $\mu = qD/k_bT$, where D is the ambipolar diffusion coefficient and q/k_bT is the thermal voltage ($\cong 26$ meV).

III. THEORETICAL PRINCIPLES

At the critical points of a semiconductor material, the PMR signal exhibits a sharp third-derivative lineshape which arises from an electromodulation effect.[9] In this case the PMR signal becomes:

$$\frac{\Delta R}{R} = \frac{2qN_e\Delta V}{\epsilon_s} \times L(\lambda). \tag{1}$$

where q is the electronic charge, N_e is the carrier concentration, ΔV is the SPV, ϵ_s is the static dielectric constant, and $L(\lambda)$ is a line-shape function determined by the semiconductor bandstructure (λ is the probe beam wavelength). Eq. (1) is valid for depleted surfaces provided the electric field is not too inhomogeneous.[9,10]

The SPV depends on the pump beam and the physics of its interaction with the sample.[1] The SPV is generally linear in the pump intensity provided the photo-injection is small with respect to the restoring current.[11,12] In this case the SPV will exhibit the spatial dependence of the excess carrier density. In the limit $\omega_p(Z) \gg L_d$, the SPV may be obtained from the solution of the one-dimensional (1D) differential equation for the modulated the carrier density.[2] In the three-dimensional (3D) limit ($\omega_p(Z) \ll L_d$), the excess carrier density involves a Hankel transform of the 1D solution and therefore must be treated numerically.[13,14] However, the use here of laser beams for both the pump and probe means the electric field of the reflected probe beam may instead be treated directly according to the analytically tractable method of Gaussian decomposition.[15–17]

Consider cylindrically symmetric Gaussian pump and probe beams directed at normal incidence onto a sample. The beams are collinear and co-focused along the z-axis. The distance between the common beam waist and the sample surface is Z. The Fresnel coefficient for the reflected probe beam includes the changes due to pump-induced energy transformation processes. The Gaussian profile of the incident pump beam is broadened by carrier diffusion in the sample. However, the mirror-reflected probe beam amplitude may be expanded as a sum of Gaussian beams of decreasing waist.[15] Given a dominant photovoltage effect according to Eq. (1), and retaining only two terms in the expansion, the electric field of the reflected probe laser beam at the surface of the sample (disregarding the common spatial phase) may be written:

$$E_r = \frac{E_o\omega_o}{\omega(Z)} \exp\left\{\frac{-\rho^2}{\omega^2(Z)}\right\} \times \left[\tilde{r} + \frac{\partial\tilde{r}}{\partial n}(n_2 + ik_2)\frac{I_p\omega_m^2}{\omega_m^2(Z)} \exp\left\{\frac{-2\rho^2}{\omega_m^2(Z)}\right\}\right] \tag{2}$$

where $|E_o|^2$ is the intensity of the probe beam at focus, ω_o is the probe beam waist (*i.e.* $\omega(Z) = \omega_o\sqrt{1+(Z/z_o)^2}$, where $z_o = \pi\omega_o^2/\lambda$ is the Rayleigh range of the probe beam), ρ is radial distance as measured from the probe beam axis, $\tilde{r}$ is the complex reflectance coefficient, n is the refractive index, I_p is the intensity of the pump beam at focus, $\omega_m(Z)$ is the radius of modulation as previously defined, and n_2 and k_2 are effective nonlinear indices defined by the coefficients appearing in Eq. (1). The leading term corresponds to the DC component of the reflected beam whereas the second term corresponds to its modulated component.

Squaring the mirror-reflected probe field and integrating the over the beam profile yields the spatially integrated PMR signal via the identification:

$$\frac{R+\Delta R}{R} = \frac{\int_0^\infty |E_r|^2 \rho d\rho}{\int_0^\infty |E_{dc}|^2 \rho d\rho} \tag{3}$$

where E_{dc} is just the linear reflectance amplitude. Neglecting terms second order in the nonlinear indices and performing the spatial integrations in Eq. (3), the PMR signal becomes:

$$\frac{\Delta R}{R} = \frac{4n_2 I_p}{n^2-1} \times \frac{\omega_p^2 + L_d^2}{\omega^2(Z) + \omega_p^2(Z) + L_d^2} \tag{4}$$

where $n^2 \gg k^2$. The key observation here is that the Z dependence of the PMR signal is contained entirely within the denominator of Eq. (4). Moreover, if $\omega_o^2+\omega_p^2 \leq L_d^2$, the 3D limit will be approached for $Z = 0$. Thus the appearance of L_d^2 in the denominator of Eq. (4) shows the Z dependence of the PMR signal will depend strongly on diffusion length provided the pump and probe beam waists are commensurate with L_d.

At intermediate frequencies where the recombination lifetime τ is comparable to the modulation period, τ likewise becomes coupled into the Z dependence of the PMR signal through the appearance of the complex diffusion length $\tilde{L}_d = L_d/\sqrt{1+i\Omega\tau}$, where Ω is the modulation frequency in radians per second. In particular, Eq. (4) demonstrates that the PMR signal as a function of Z may be parameterized by the expression:

$$\frac{\Delta R}{R} = \frac{A\exp i\phi_o}{\omega^2(Z) + \omega_p^2(Z) + \tilde{L}_d^2} \tag{5}$$

where A and ϕ_o are the Z independent amplitude and phase, respectively.

The coupling of $\tilde{L}_d$ into the Z-dependence of the PMR signal indicates that L_d, and ultimately τ, may be determined by a regressive fit to the experimental Z-scan PMR data. For example, according to Eq. (5), the Z dependence of the PMR amplitude may be simply parameterized by the set of variables: A, L_d^2, ω_p^2, ω_o^2, and $\Omega\tau$, whereas the corresponding phase expression allows parametrization using the variables: ϕ_o, L_d^2, ω_p^2, ω_o^2, and $\Omega\tau$. (Note that Ω, ω_o, and ω_p are fixed by the system.) In the 3D limit the PMR amplitude becomes independent of $\Omega\tau$, whereas the PMR phase becomes independent of L_d^2. Thus, provided the 3D limit is approached, an iterative procedure involving independent nonlinear fits to the amplitude and phase expressions may be used to establish L_d and τ and their statistical uncertainties. For example, the analytic expression for the phase may first be used to provide an independent estimate of τ and its uncertainty.[18] Then the output value for τ may be held constant in the amplitude fit in order to estimate L_d and its uncertainty.

IV. EXPERIMENT AND DISCUSSION

In order to test the capability of the Z-scan PMR technique to measure the effect of systematic process variations on carrier mobility, a set of samples with various p-type ultra shallow junctions were formed in silicon (100) substrates. The substrates were implanted with n-type counter-dopant (As) followed by low-energy high-dose B implantation. Dopant activation was performed using millisecond timescale flash-lamp based annealing. A range of base temperature and flash temperature targets were used to study dopant activation, implanted dopant diffusion, and material quality. The process conditions studied included: (i) flash target temperatures in the $1250-1350$°C range, (ii) an additional thermal annealing of the As counter-doping layer prior to B implantation, and (iii) use of a Ge amorphizing implant (AI) to reduce B ion channeling. The AI process introduces a layer of crystalline defects close to the sample surface. These defects reduce the carrier diffusion length and recombination time in the implanted region. SIMS data indicated post-activation B doping levels of $\approx 1\times10^{19}$/cc at $X_j \cong 20$ nm across the sample set. The conventional 1D Poisson analysis estimates junction voltages on the order of several volts.

The experimental PMR apparatus used was similar to an instrument described elsewhere.[19] The laser pump and probe beams were produced with milliwatt power semiconductor diode lasers. The pump was amplitude modulated via a reference signal from the lock-in amplifier. The pump and probe wavelengths were 488 and 375 nm, respectively. The pump light has an absorption depth in Si of $\approx$ 500 nm. The wavelength of the probe beam was chosen near the lowest energy direct interband transition in Si, resulting in a dominant photovoltage effect. The optical absorption depth in Si at 375 nm is $\cong$ 23 nm. Therefore, any detected photo-voltage must occur at or near the surface.[10] The pump and probe beams were co-focused to an ≈ 2 μm radius on the ultra-shallow shallow junction samples. Neutral density filters at the laser outputs were used to maintain low photo-injection at focus.[20] The entire reflected probe beam was collected and focused onto the detector, thus radially integrating the beam. In general, the phase in a modulated SPV measurement will exhibit a linear dependence upon Ω in the intermediate regime.[12] For each of the wafers used

TABLE I. Measured carrier diffusion lengths, recombination times and mobilities, as determined via fitting to Z-scan PMR data obtained from the subset of samples that received amorphizing implant.

	L_d [μm]		τ [ns]		μ [cm^2/V $\cdot$ s]	
Flash temp [°C]	Flash only	As pre-soak	Flash only	As pre-soak	Flash only	As pre-soak
1300/550	6.07 ± 0.02	6.01 ± 0.02	90.5 ± 0.5	87.6 ± 0.6	157 ± 2	159 ± 2
1300/550($2X$)	9.09 ± 0.03	8.63 ± 0.02	83.1 ± 0.4	67.0 ± 0.5	382 ± 4	427 ± 5
1300/600	9.36 ± 0.08	9.92 ± 0.08	159.9 ± 0.5	167.3 ± 0.5	211 ± 3	226 ± 4
1350/600	10.19 ± 0.05	11.68 ± 0.02	163.0 ± 0.5	167.9 ± 0.5	245 ± 4	312 ± 4

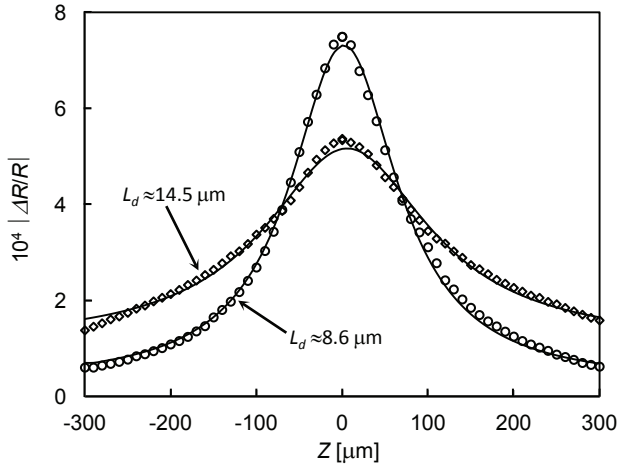

FIG. 2. Z-scan PMR amplitude data and fits showing the effect of near surface damage (due to AI) on shallow electrical junctions formed in silicon. The more narrow Z profile indicates a shorter diffusion length.

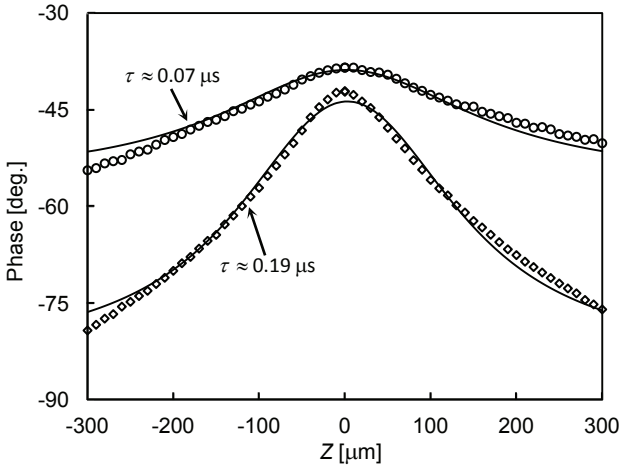

FIG. 3. Z-scan PMR phase data from the same pair of samples as shown in Fig. 2, again showing the effect of near surface damage (due to AI) on the junction. The broader Z profile indicates a shorter recombination lifetime.

in this study, this linearity was confirmed over the frequency range $600 - 900$ kHz. Thus an optimal modulation frequency of 750 kHz was selected. The samples were stepped through focus and the Z-scan PMR data was recorded. Estimates for $\Omega\tau$ were obtained via regressive fitting to the phase data. Then $\Omega\tau$ was fixed in regressive fits to the amplitude data in order to yield L_d^2. The estimated uncertainties in the extracted parameters were also output from the fitting procedure.

Fig. 2 shows experimental Z-scan PMR amplitude data and fits obtained from samples with and without AI. The more sharply peaked PMR response as a function of Z seen on the sample with AI evidences a shorter diffusion length. This behavior was apparent in the raw data for all samples that received the AI process. Fig. 3 shows experimental Z-scan PMR phase data and fit obtained from the same pair of samples as shown in Fig. 2. Note the more sharply peaked amplitude data corresponds to the broader phase data. The mobility and its estimated uncertainty were obtained from the extracted parameters via the Einstein relation. Table 1 lists fitted values of diffusion length, recombination time, and mobility for the subset of samples with AI, assuming a measurement uncertainty of 2 ppm for the PMR amplitude and 0.13° for the PMR phase.

Systematic variations in the measured carrier parameters with process conditions are observed. Overall, the measured parameters show little sensitivity to the As thermal anneal (columns labeled "As pre-soak"). When the 1300°C/550°C flash anneal is repeated, the diffusion length increases by a factor of $\approx 1.5X$, indicating the onset of junction activation. When the base temperature of the flash anneal is increased to 600°C, the recombination time roughly doubles, indicating better removal of the AI damage. Thus the effects of the process variations investigated here on carrier transport properties are readily observed. The measured mobilities were found to be in reasonable agreement with literature values corresponding to the activated doping levels. For all samples tested, estimated statistical uncertainty in the extracted mobility remains less than 2%.

The Z-scan PMR technique presented here has been used to measure carrier transport properties with high precision using data obtained from a convenient optical arrangement. The technique is suitable for making non-contact process control measurements and thus addresses a key outstanding need in semiconductor manufacturing. Current work is underway to expand the range of transport properties accessible via the technique.

[1]L. Kronik and Y. Shapira, Surf. Sci. Rep. **37**, 1 (1999), doi:10.1016/S0167-5729(99)00002-3.
[2]D. K. Schroder, Meas. Sci. Technol. **12**, R16 (2001), doi:10.1088/0957-0233/12/3/202.
[3]H.-J. Schulze, A. Frohnmeyer, F.-J. Niedernostheide, F. Hille, P. Tutto, T. Pavelka, and G. Wachutka, J. Electrochem. Soc. **148**, G655 (2001), doi:10.1149/1.1409974.
[4]D. Baek, S. Rouvimov, B. Kim, T.-C. Jo, and D. K. Schroder, Appl. Phys. Lett. **86**, 112110 (2005), doi:10.1063/1.1884258.
[5]R. Ulbricht, E. Hendry, J. Shan, T. F. Heinz, and M. Bonn, Rev. Mod. Phys. **83**, 543 (2011), doi:10.1103/RevModPhys.83.543.
[6]B. G. Alberding, W. R. Thurber, and E. J. Heilweil, J. Opt. Soc. Am. B **34**, 1392 (2017), doi:10.1364/JOSAB.34.001392.
[7]F. H. Pollak, in *Optical Properties of Semiconductors*, Handbook of Semiconductors, Vol. 2, edited by M. Balkanski (North-Holland, Amsterdam, 1994) Chap. 10.
[8]A. Mandelis, in *Diffusion-Wave Fields: Mathematical Methods and Green Functions* (Springer, New York, 2001) Chap. 9, pp. 626–627.
[9]D. E. Aspnes, Phys. Rev. Lett. **28**, 913 (1972), doi:10.1103/PhysRevLett.28.913.
[10]D. E. Aspnes and A. Frova, Solid State Comm. **7**, 155 (1969), doi:10.1016/0038-1098(69)90714-5.
[11]D. K. Schroder, IEEE Trans. Electron Devices **44**, 160 (1997), doi:10.1109/16.554806.
[12]J. E. Park, D. K. Schroder, S. E. Tan, B. D. Choi, M. Fletcher, A. Buczkowski, and F. Kirscht, J. Electrochem. Soc. **148**, G411 (2001), doi:10.1149/1.1380257.
[13]J. Opsal, A. Rosencwaig, and D. L. Willenborg, Appl. Opt. **22**, 3169 (1983), doi:10.1364/AO.22.003169.
[14]J. Opsal, M. W. Taylor, W. L. Smith, and A. Rosenwaig, J. Appl. Phys. **61**, 240 (1987), doi:10.1063/1.338863.
[15]D. Weaire, B. S. Wherrett, D. A. B. Miller, and S. D. Smith, Opt. Lett. **4**, 331 (1979), doi:10.1364/OL.4.000331.
[16]M. Sheik-Bahae, A. A. Said, and E. W. van Stryland, Opt. Lett. **14**, 955 (1989), doi:10.1364/OL.14.000955.
[17]D. V. Petrov, A. S. L. Gomes, and C. B. de Araujo, Appl. Phys. Lett. **65**, 1067 (1994), doi:10.1063/1.112175.
[18]W. H. Press, S. A. Teukolsky, W. T. Vetterling, and B. P. Flannery, in *Numerical Recipes in Fortran 77: The Art of Scientific Computing*, Fortran Numerical Recipes, Vol. 1 (Cambridge University Press, New York, 1996) 2nd ed., Chap. 15.
[19]W. Chism and J. Cartwright, Thin Solid Films **520**, 6521 (2012), doi:10.1016/j.tsf.2012.06.065.
[20]W. Chism, M. Current, and V. Vartanian, J. Vac. Sci. Technol. B **28**, C1C15 (2010), doi:10.1116/1.3253327.